Toward a Surface Science Model for Biology: Glycine Adsorption on Nanohydroxyapatite with Well-Defined Surfaces

ARTICLE *in* JOURNAL OF PHYSICAL CHEMISTRY LETTERS · JUNE 2011

Impact Factor: 7.46 · DOI: 10.1021/jz200457x

6 AUTHORS, INCLUDING:

Yu. Sakhno
Università degli Studi di Torino
27 PUBLICATIONS **110** CITATIONS
SEE PROFILE

Luca Bertinetti
Max Planck Institute of Colloids and Interfaces
68 PUBLICATIONS **916** CITATIONS
SEE PROFILE

Gianmario Martra
Università degli Studi di Torino
244 PUBLICATIONS **5,523** CITATIONS
SEE PROFILE

Piero Ugliengo
Università degli Studi di Torino
244 PUBLICATIONS **6,115** CITATIONS
SEE PROFILE

THE JOURNAL OF PHYSICAL CHEMISTRY Letters

LETTER

pubs.acs.org/JPCL

Toward a Surface Science Model for Biology: Glycine Adsorption on Nanohydroxyapatite with Well-Defined Surfaces

Albert Rimola,[†,‡] Yuriy Sakhno,[†] Luca Bertinetti,[†] Marco Lelli,[§] Gianmario Martra,[†] and Piero Ugliengo*[,†]

[†]Dipartimento di Chimica IFM & NIS Center of Excellence, Università di Torino, Via P. Giuria 7, 10125, Torino, Italy

[‡]Department de Química, Universitat Autònoma de Barcelona, 08193, Bellaterra, Spain

[§]Dipartimento di Chimica "G. Ciamician", Università di Bologna, Via Selmi 2, 40126, Bologna, Italy

Supporting Information

ABSTRACT: The adsorption by chemical vapor deposition of glycine to nanohydroxyapatite, well characterized by electron microscopy, has been studied by infrared spectroscopy and density functional theory based on the B3LYP functional. The comparison of the IR features of the adsorbed glycine with that resulting from the modeling has allowed elucidating the structures assumed by glycine at the crystalline faces of nanohydroxyapatite. These results will improve the understanding of the biomolecules/biomaterials interactions.

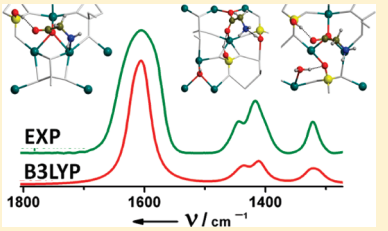

SECTION: Surfaces, Interfaces, Catalysis

Hydroxyapatite (HA), $[Ca_{10}(PO_4)_6(OH)_2]$, the natural major inorganic constituent of bone and teeth in the form of nanocrystals, is usually a system of choice to study protein/biocompatible-surface interactions. The study of these interactions is crucial not only for the development of new biomaterials[1] and to understand biomineralization processes[2] but also for several technological and biomedical applications[3−5] such as biodevices[6] and drug delivery systems.[7] Nonetheless, despite the great efforts in investigating protein/HA systems,[8−11] atomistic information on the actual contact occurring at the interface is rather scarce. Suitable to this target is the adoption of a "surface science model" approach,[12] based on the interplay among the preparation of materials with well-defined surface features and spectroscopic and accurate quantum mechanical techniques. This approach has been very fruitful to obtain a deep knowledge of surface molecular events relevant for heterogeneous catalysis, hence successfully developing a well-established "surface science model for catalysis".[13,14] In that respect, it is worth pointing out that for the model to be successful, extended nondefective crystalline faces grown out of a single crystal are usually employed, together with ultrahigh vacuum conditions. At variance with this approach, here we worked at standard conditions and focused on the possibility of employing nanometric HA particles with well-defined surfaces, because in bone tissues, HA is present as nanoparticles embedded in a collagen matrix[15−21] to form a highly organized composite material and not as a bulk extended crystal.[22] This has stimulated several researchers to develop methods to prepare HA in nanosized forms, which actually exhibit improved in vitro performance when tested with osteoblasts.[23,24] In this respect, it was recently possible to grow highly crystalline HA nanoparticles with platelet morphology,[25] exposing (010) planes as basal surfaces (with sides in the 40−100 nm range), and (001) and (100) planes (the latter being isostructural with the (010) one) as lateral terminations (ca. 5−10 nm) (Figure 1; textural and structural data in the Supporting Information (SI), Table SI-1 and Figure SI-1). In particular, it can be clearly seen that the phase contrast fringes extend up to the boundary of the particles, indicating that the crystalline order reached the particle surface, where regular patterns of calcium and phosphate should be exposed. Furthermore, the homogeneity of the phase contrast of the image of HA-crystals observed along the [010] zone axis indicates a constant thickness of the material in the direction perpendicular to the image plane.

Here, these HA nanoparticles were used to investigate the adsorption of nonionic $HOOC-CH_2-NH_2$ glycine (Gly) vapors (see SI, scheme SI-1) by means of IR measurements. The adoption of a single aminoacid, as the basic molecular brick of proteins, has allowed researchers to supplement the experimental measurements with modeling techniques based on first-principle quantum mechanical methods that have been successfully adopted in the past by some of us.[26−29] The adsorption of a real protein as a whole, while in principle desirable, would hinder, due to its size, an accurate modeling of the protein/HA interactions. In fact, only molecular mechanics and dynamics using force fields (FFs) have been reported in this case.[30−34] The present FFs cannot provide accurate results, as they cannot cope with chemical reactions that may occur between the adsorbate and the HA surface functionalities. These reactions are common, as is the case even for the simple water molecule adsorbed at the pristine (010) stoichiometric HA surface.[35] Furthermore, the accuracy of the FF interaction energies of proteins/HA surfaces are hard to assess due to the paucity of accurate structural and energetic experimental measurements.

Received: April 6, 2011
Accepted: May 20, 2011
Published: May 20, 2011

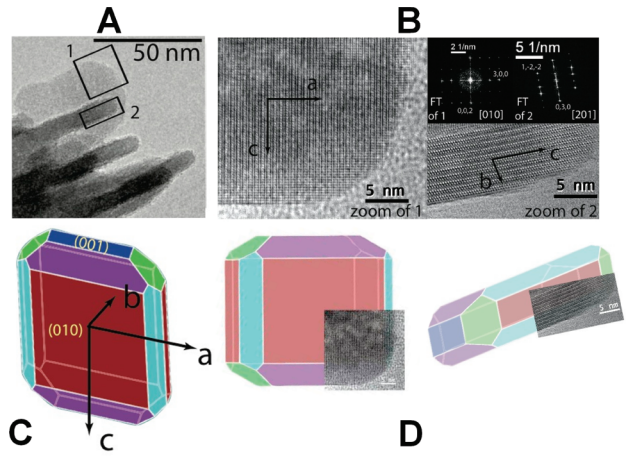

Figure 1. Transmission electron microscopy (TEM) images representative of the morphology (A) and surface structure (B) of the hydroxyapatite nanoparticles used in this study. Upper-right panel: Fourier transform (FT) of the high resolution images, indicating that surfaces projected on the image plane of zoom 1 and 2 are of the (010) and (100) type, respectively. Further details are in ref 25. C and D are three-dimensional schemes of HA particles, highlighting the extension along the crystallographic axes, the indexing of main surface planes, and the correspondence with the two-dimensional high-resolution images in panel B.

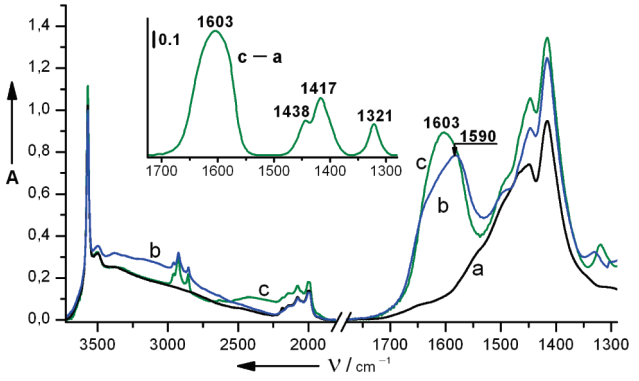

Figure 2. IR spectra of HA: (a) preoutgassed at 433 K for 1 h, (b) at the end of the stepwise adsorption of Gly from the vapor phase, and (c) after subsequent D_2O adsorption/desorption cycles (until attainment of invariance of spectra). Spectra (b) and (c) were collected after a further outgassing at beam temperature (b.t., ca. 323 K) for 1 h. Inset: result of the subtraction of spectrum (a) from spectrum (c), in the 1710−1290 cm^{-1} range.

The spectra corresponding to bare HA (bands assignment in SI, Figure SI-2) and to the highest amount of adsorbed Gly, exhibiting an intensity close to that expected for a coverage of 1 Gly molecule/nm^2 (below the monolayer, see Figure SI-3 in theSI) are displayed in Figure 2 (curves a and b, respectively). Spectra collected during the stepwise Gly adsorption and insights on the effectiveness of such procedure are reported in the SI, Figures SI-3A and SI-4.

The adsorption of Gly results in the appearance of a broad band spread over the 3500−2250 cm^{-1} range, due to stretching modes of H-bonded N−H_x groups, with overimposed narrower components due to the ν(CH) modes, and of a main peak with a maximum at 1590 cm^{-1}, whose asymmetry indicates the presence of various sub-bands. Other less intense components at

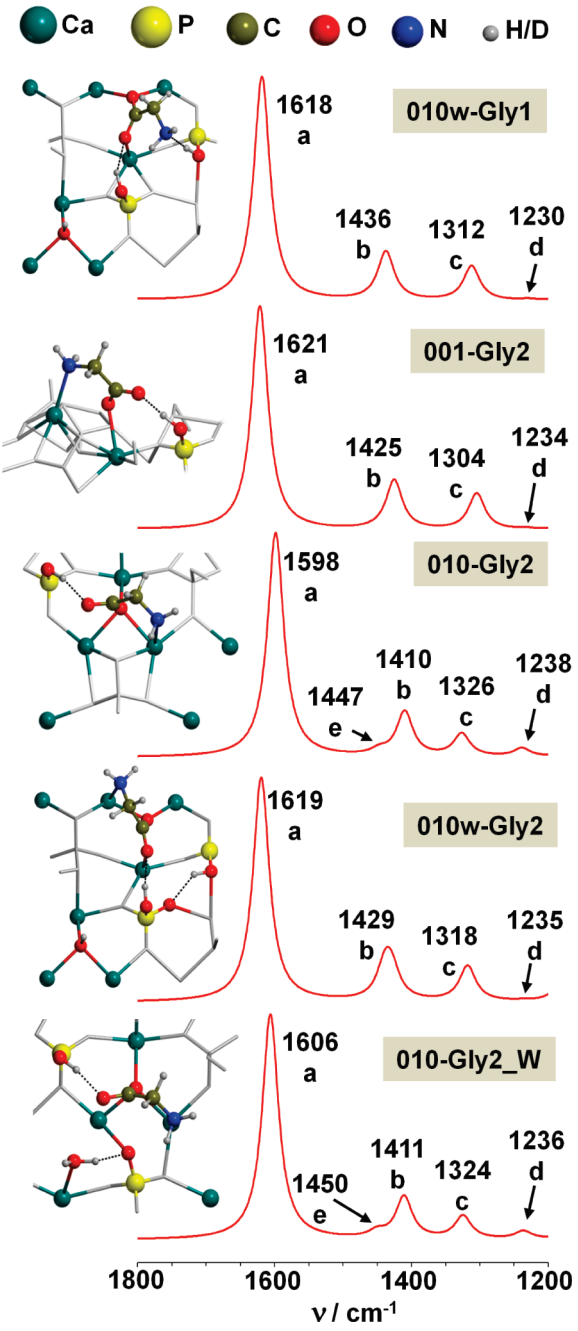

Figure 3. Scaled B3LYP harmonic infrared spectra. Band labels are as follows: (a) $\nu(COO^-)$a; (b) $\boldsymbol{\nu(COO-)s} + \delta(CCH)$; (c) $\boldsymbol{\delta(CCH)} + \nu(COO^-)$s; (d) $\gamma(CH_2)$; (e) $\delta(CH_2)$. For b and c, modes in bold are dominant.

1550−1350 cm^{-1} and a minor band at 1336 cm^{-1} are also observed. The spectral profile due to adsorbed Gly, obtained by subtraction of bare HA, is reported in the inset of Figure SI-3A. As $-NH_2$ and $-NH_3^+$ groups are known to exhibit deformation bands in the 1650−1550 cm^{-1} region,[36] to simplify the pattern and allow a more detailed analysis, a H/D exchange at the amino moiety was carried out by contact with D_2O, followed by outgassing at room temperature (Figure 2, curve c). The main band at 1590 cm^{-1} is transformed in a more symmetric and narrower signal with a maximum at 1603 cm^{-1}, the components due to the amino groups being downshifted below 1200 cm^{-1}.[37]

dx.doi.org/10.1021/jz200457x |J. Phys. Chem. Lett. 2011, 2, 1390–1394

The observed increase in intensity is proposed to be due to the intensity stealing/borrowing of modes localized on the carboxylic and amino moieties (see SI, Figure SI-5). Conversely, the component in the 2750−2000 cm^{-1} range still appeared too broad to easily extract the part due to ν(ND) modes. The spectral profile in the 1800−1250 cm^{-1} region of the deuterated adsorbed Gly was more clearly appreciated after subtraction of the spectrum of the bare HA sample (Figure 2, inset). The squat shape of the main signal at 1603 cm^{-1} (impossible to fit with a single band, independently of the Gaussian/Lorentzian ratio adopted for the fitting), clearly suggests the presence of sub-bands, likely related to surface adducts different in nature/structure.

Periodic B3LYP calculations with a polarized double-ζ basis set using the CRYSTAL06 code[38] have then been carried out to provide structures and energetic and IR spectra of different possible Gly adducts on a (010) HA surface (see SI, Figure SI-6A), by analogy with the most extended surfaces of the HA nanoparticles employed. Furthermore, the (010) surface reacted with water (referred to as 010w; see SI, Figure SI-6B), spontaneously formed when water adsorbs on the pristine (010) surface,[35] was also considered. Such surface is then representative of the portions of the surface of the HA particles bearing some hydroxy groups,[25] likely resulting from the growth of HA nanoparticles in an aqueous medium. Moreover, the (001) HA surface was also taken into account (see SI, Figure SI-6C). As for the amino acid, all exchangeable H atoms in both Gly and HA model surfaces were substituted with D atoms, for the sake of comparison. As stated in a previous work done by some of us,[26] Gly coming from the vapor phase is first converted to Gly^-/HA^+ ion pairs (Gly2-type structures) by proton transfer, which can then evolve in the more stable Gly1-type forms. The simulated IR spectra of the 001-Gly1 and 010-Gly1 adducts do not match well with the experimental spectrum (see SI, Figure SI-7) as the highest frequency features appear at too high frequency compared to the experiment. Furthermore, the {001} form is a rather minor feature of the HA nanocrystals so that the contribution to the final spectrum coming from Gly on the (001) surfaces should be less relevant than for the well developed {010} form. Contrarily, the computed $\nu(COO^-)$a value of 010w-Gly1 is closer to the experimental one (see Figure 3) due to the H-bond between the COO^- group and the surface proton derived from the dissociated water. In the second most stable complexes (Gly2-type), Gly deprotonates spontaneously, giving a strong H-bond between the COO^- group and the formed P-OD surface group (see 001-Gly2, 010-Gly2 and 010w-Gly2 of Figure SI-8 in theSI). As a consequence, the $\nu(COO^-)$a modes are bathochromically shifted, and the values obtained in the simulated IR spectra (see Figure 3) are in reasonable agreement with the experiment. As for the amino group, a coordinative interaction with a Ca^{2+} ion through the lone pair of the N atom occurs. Finally, as H_2O and then D_2O were sent on the Gly/HA sample at the end of the adsorption process (see above), we have included one heavy water molecule in some of the Gly/HA models (see 001-Gly2_W and 010-Gly2_W of Figure SI-9 in the SI). The simulated spectra for these two structures indicate that, whereas the former complex shows a $\nu(COO^-)$a vibrational mode that is exceedingly low (1555 cm^{-1}) because the additional water strengthens the $COO^-\cdots$DO-P H-bond, in the latter the $\nu(COO^-)$a matches (1606 cm^{-1}) with the experimental value (see Figure 3).

Although there are five Gly/HA complexes that match reasonably well with the main $\nu(COO^-)$a experimental band, no single computed spectrum fits the experimental profile (inset of Figure 2)

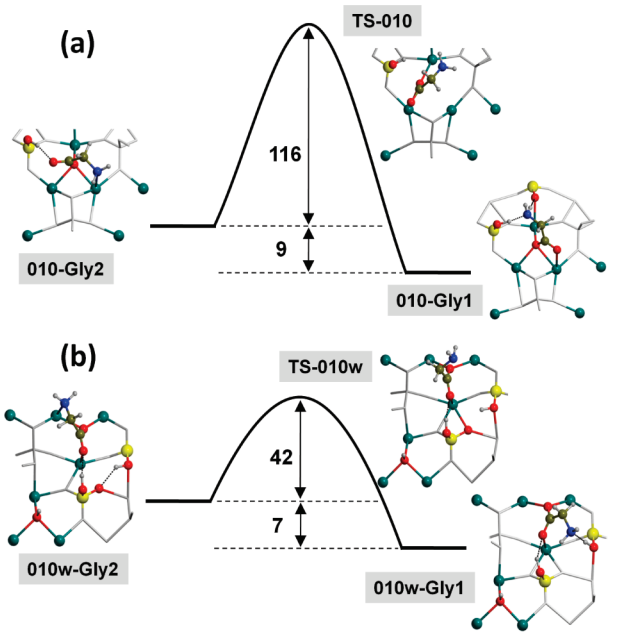

Figure 4. B3LYP potential energy surface for (a) 010-Gly2→010-Gly1 and (b) 010w-Gly2→010w-Gly1 reactions. Values are in units of kJ mol^{-1}.

well enough: this suggests that at least three spectra are expected to contribute to the final spectrum, as the squat shape of the experimental band at around 1600 cm^{-1} cannot be represented with less than three components, as is the case for the spectral features at lower frequencies. Therefore, we have built spectrum profiles by summation of the absolute intensities of the five different simulated spectra of Figure 3, taking into account all possible combinations (see SI, Figure SI-10). What remains to be decided is the relative weight associated with the IR intensity of each of the three spectrum adopted to build up the final one. The mathematical features of the experimental band at around 1600 cm^{-1} suggest that the three spectra should appear with almost the same weight (1:1:1) in order to properly reproduce the squat shape and the broadness of the band. This choice is also the simplest one among other more involved combinations. It is then found that two of them, i.e., 010w-Gly1+010-Gly2+010-Gly2_W and 010w-Gly2+010-Gly2+010-Gly2_W, are in good agreement with the experimental profile. To narrow the choice, energetic features of the conversion from Gly2-type to Gly1-type were considered.

Details of these processes are shown by the computed energy profiles of the 010-Gly2 → 010-Gly1 and 010w-Gly2 → 010w-Gly1 steps, including the characterization of the transition state points.[39] Figure 4 shows that the energy barriers for the first and second process are 116 and 42 kJ mol^{-1}, respectively. The two barriers differ because the 010-Gly2 → 010-Gly1 conversion requires the breaking of two strong interactions (i.e., $COO^-\cdots$D-OP and the $Ca\cdots$N bonds), whereas only one (the $Ca\cdots$N bond) needs to be broken for the 010w-Gly2 → 010w-Gly1 conversion. This means that, while 010w-Gly2 will convert to the most stable 010w-Gly1 structure, 010-Gly2 will stay as such. For the 010-Gly2_W case, a high barrier is expected (as for the 010-Gly2 case), as the extra water only acts as a silent coadsorbate during the conversion. We are aware that the processes described in Figure 4 are an oversimplified view of what may happen on the real material, particularly when H_2O/D_2O exchange experiment was carried out. A key question would be to see whether H_2O

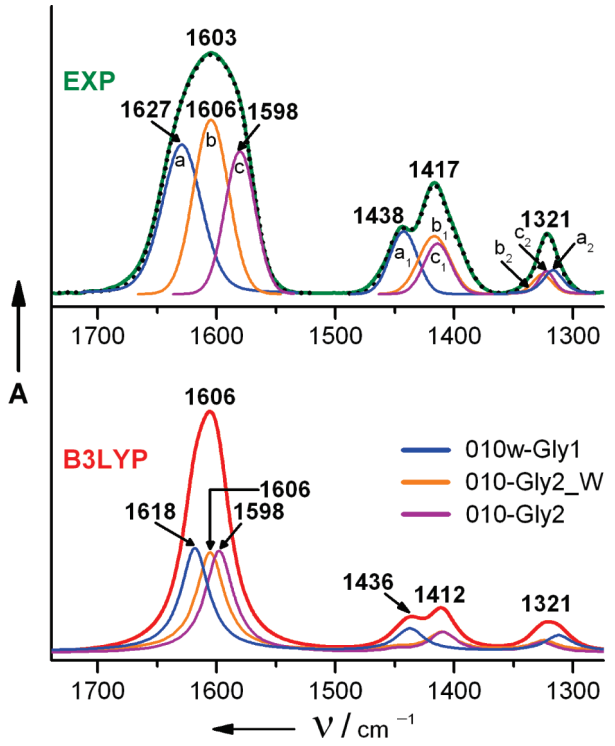

Figure 5. Experimental and simulated IR spectra of Gly adsorbed from the vapor phase on HA, reported in the 1740−1275 cm^{-1} region. The simulated spectra (in red) results from the contribution of three Gly/HA adducts: 010w-Gly1 (blue), 010-Gly2_W (orange), and 010-Gly2 (purple); see text for details. The experimental spectrum (solid green line), is the same trace reported in the inset of Figure 2. The dotted profile superimposed to the experimental spectrum is the result of the summation of the components obtained by the fitting procedure, displayed as colored dotted curves below the spectrum. Components labeled with the same letters (e.g, a, a1, a2) refer to the same adsorbed species.

may change the energy profiles in any relevant way. A possible answer, without resorting to very time-consuming calculations, comes from recent work by some of us on the competition between Gly and H_2O at the HA surfaces.[28] It was indeed found that Gly prefers to directly interact with the HA surface, the preadsorbed H_2O being displaced by Gly and decorating the remaining available sites as in structure 010-Gly2_W. This suggests that the strong interactions responsible of the kinetic barriers remain almost the same despite the presence of H_2O, which will alter in a systematic way the position of the stationary points with little changes in the relative energies. By assuming that, the simulated spectra of the best candidate 010w-Gly1, 010-Gly2, 010-Gly2_W adducts were used as guidelines to the deconvolution of the experimental one by using only three main components, and an excellent agreement was found (Figure 5). Notwithstanding, minor contribution from other species, formed on different and less abundant surface terminations, cannot be excluded. In particular, this should be the case for the component *a*, which exhibits both the largest discrepancy with respect to the calculated position and width at half-maximum.

The combination between experimental spectroscopic techniques and atomistic quantum mechanical calculations based on accurate hybrid functionals has shown that the well-established "surface science model for catalysis" can be extended toward an effective "surface science model for biology"[12] even in the case of well-shaped biomaterial nanoparticles. Despite the functionalities of Gly, being the simplest aminoacid, it will not be present when embedded in a protein, thus the COOH and NH_2 groups studied here are the prototypes for the lateral chains of glutamic acid and lysine, respectively. The same methodology adopted here can be straightforwardly extended to study other amino acids, provided their ability to sublimate before decomposing.[40] Nevertheless, we are aware that more work is needed to study adsorbate of larger size (i.e., oligopeptides) and to understand the role of water. Indeed, these steps have been planned to be the subject of future work in our laboratory.

■ ASSOCIATED CONTENT

Supporting Information. Materials, experimental procedure, computational details, and additional Figures and Tables. This material is available free of charge via the Internet at http://pubs.acs.org.

■ AUTHOR INFORMATION

Corresponding Author

*Tel: +39-011-6704596. Fax: +39-011-2364596. E-mail: piero.ugliengo@unito.it.

■ ACKNOWLEDGMENT

A.R. is indebted to "Comissionat per a Universitats i Recerca del Departament d'Innovació, Universitats i Empresa de la Generalitat de Catalunya". Financial support from MICINN, through the CTQ2008-06381/BQU project is gratefully acknowledged. Some of the largest calculations of this work have been supported by generous allowance of computer time from the Barcelona Supercomputing Centre (Projects: BCV-2008-2-0013; BCV-2008-3-0006: Simulation of peptide folding induced by inorganic materials) and the CINECA computing centre. S. Coluccia, M. Corno (Dip. Chimica IFM, University of Torino), and N. Roveri (Dip. Chimica, University of Bologna) are acknowledged for fruitful discussion.

■ REFERENCES

(1) Hench, L. L.; Polak, J. M. Third-Generation Biomedical Materials. *Science* **2002**, *295* (5557), 1014–1017.

(2) Estroff, L. A. Introduction: Biomineralization. *Chem. Rev.* **2008**, *108* (11), 4329–4331and all articles included in this special issue "Biomineralization".

(3) Gray, J. J. The Interaction of Proteins with Solid Surfaces. *Curr. Opin. Struct. Biol.* **2004**, *14* (1), 110–115.

(4) Vo-Dinh, T., *Nanotechnology in Biology and Medicine: Methods, Devices, and Applications*; Taylor & Francis Group: Boca Raton, FL, 2007.

(5) Bachmann, M.; Goede, K.; Beck-Sickinger, A. G.; Grundmann, M.; Irback, A.; Janke, W. Microscopic Mechanism of Specific Peptide Adhesion to Semiconductor Substrate. *Angew. Chem., Int. Ed.* **2010**, *49*, 9530–9533.

(6) Schröder, E.; Jönsson, T.; Poole, L. Hydroxyapatite Chromatography: Altering the Phosphate-Dependent Elution Profile of Protein as a Function of pH. *Anal. Biochem.* **2003**, *313* (1), 176–178.

(7) Vallet-Regí, M. Ordered Mesoporous Materials in the Context of Drug Delivery Systems and Bone Tissue Engineering. *Chem.—Eur. J.* **2006**, *12* (23), 5934–5943.

(8) Goobes, G.; Goobes, R.; Shaw, W. J.; Gibson, J. M.; Long, J. R.; Raghunathan, V.; Schueler-Furman, O.; Popham, J. M.; Baker, D.; Campbell, C. T.; et al. The Structure, Dynamics, and Energetics of Protein Adsorption − Lessons Learned from Adsorption of Statherin to

Hydroxyapatite. *Magn. Reson. Chem.* **2007**, *45*, S32–S47and references therein.

(9) Lee, J. S.; Lee, J. S.; Wagoner-Johnson, A.; Murphy, W. L. Modular Peptide Growth Factors for Substrate-Mediated Stem Cell Differentiation. *Angew. Chem., Int. Ed.* **2009**, *48*, 6266–6269.

(10) Makrodimitris, K.; Masica, D. L.; Kim, E. T.; Gray, J. J. Structure Prediction of Protein−Solid Surface Interactions Reveals a Molecular Recognition Motif of Statherin fo Hydroxyapatite. *J. Am. Chem. Soc.* **2007**, *129*, 13713–13722.

(11) Sarikaya, M.; Tamerler, C.; Jen, A. K.-Y.; Schulten, K.; Baneyx, F. Molecular Biomimetics: Nanotechnology Through Biology. *Nat. Mater.* **2003**, *2*, 577–585.

(12) Castner, D. G.; Ratner, B. D. Biomedical Surface Science: Foundations to Frontiers. *Surf. Sci.* **2002**, *500* (1−3), 28–60.

(13) Ertl, G. Dynamics of Reactions at Surfaces. *Adv. Catal.* **2000**, *45*, 1–69.

(14) Hammer, B.; Norskov, J. K. Theoretical Surface Science and Catalysis. Calculations and Concepts. *Adv. Catal.* **2000**, *45*, 71–129.

(15) Streeter, I.; de Leeuw, N. H. Atomistic Modeling of Collagen Proteins in Their Fibrillar Environment. *J. Phys. Chem. B* **2010**, *114*, 13263–13270.

(16) Katti, D. R.; Pradhan, S. M.; Katti, K. S. Directional Dependence of Hydroxyapatite-Collagen Interactions on Mechanics of Collagen. *J. Biomechanics* **2010**, *43*, 1723–1730.

(17) Bhowmik, R.; Katti, K.; Katti, D. Mechanics of Molecular Collagen is Influenced by Hydroxyapatite in Natural Bone. *J. Mat. Science* **2007**, *42*, 8795–8803.

(18) Bhowmik, R.; Katti, K. S.; Katti, D. R. Mechanisms of Load-Deformation Behavior of Molecular Collagen in Hydroxyapatite−Tropocollagen Molecular System: Steered Molecular Dynamics Study. *J. Eng. Mech.* **2009**, *135*, 413–421.

(19) Gautieri, A.; Russo, A.; Vesentini, S.; Redaelli, A.; Buehler, M. J. Coarse-Grained Model of Collagen Molecules Using an Extended MARTINI Force Field. *J. Chem. Theory Comput.* **2010**, *6*, 1210–1218.

(20) Buehler, M. J. Molecular Nanomechanics of Nascent Bone: Fibrillar Toughening by Mineralization. *Nanotechnology* **2007**, *18*, 295102.

(21) Dubey, D. K.; Tomar, V. Role of Molecular Level Interfacial Forces in Hard Biomaterial Mechanics: A Review. *Anna. Biomed. Eng.* **2010**, *38*, 2040–2055.

(22) Lowenstam, H. A.; Weiner, S. *On Biomineralization*; Oxford University Press: New York, 1989.

(23) Webster, T. J.; Ergun, C.; Doremus, R. H.; Siegel, R. W.; Bizios, R. Enhanced Functions of Osteoblasts on Nanophase Ceramics. *Biomaterials* **2000**, *21*, 1803–1810.

(24) Webster, T. J.; Ergun, C.; Doremus, R. H.; Siegel, R. W.; Bizios, R. Enhanced Osteoclast-like Cell Functions on Nanophase Ceramics. *Biomaterials* **2001**, *22*, 1327–1333.

(25) Sakhno, Y.; Bertinetti, L.; Iafisco, M.; Tampieri, A.; Roveri, N.; Martra, G. Surface Hydration and Cationic Sites of Nanohydroxyapatites with Amorphous or Crystalline Surfaces: A Comparative Study. *J. Phys. Chem. C* **2010**, *114*, 16640–16648.

(26) Rimola, A.; Corno, M.; Zicovich-Wilson, C.; Ugliengo, P. Ab-Initio Modelling of Protein/Biomaterial Interactions: Glycine Adsorption at Hydroxyapatite Surfaces. *J. Am. Chem. Soc.* **2008**, *130*, 16181–16183.

(27) Almora-Barrios, N.; Austen, K. F.; de Leeuw, N. H. Density Functional Theory Study of the Binding of Glycine, Proline, and Hydroxyproline to the Hydroxyapatite (0001) and (010) Surfaces. *Langmuir* **2009**, *25*, 5018–5025.

(28) Rimola, A.; Corno, M.; Zicovich-Wilson, C. M.; Ugliengo, P. Ab Initio Modeling of Protein/Biomaterial Interactions: Competitive Adsorption Between Glycine and Water onto Hydroxyapatite Surfaces. *Phys. Chem. Chem. Phys.* **2009**, *11*, 9005–9007.

(29) Corno, M.; Rimola, A.; Bolis, V.; Ugliengo, P. Hydroxyapatite as a Key Biomaterial: Quantum-Mechanical Simulation of its Surfaces in Interaction with Biomolecules. *Phys. Chem. Chem. Phys.* **2010**, *12*, 6309–6329.

(30) Shen, J.; Wu, T.; Wang, Q.; Pan, H. Molecular Simulation of Protein Adsorption and Desorption on Hydroxyapatite Surfaces. *Biomaterials* **2008**, *29*, 513–532.

(31) Chen, X.; Wang, Q.; Shen, J.; Pan, H.; Wu, T. Adsorption of Leucine-Rich Amelogenin Protein on Hydroxyapatite (001) Surface through −COO− Claws. *J. Phys. Chem. C* **2007**, *111*, 1284–1290.

(32) Chen, P.-H.; Tseng, Y.-H.; Mou, Y.; Tsai, Y.-L.; Guo, S.-M.; Huang, S.-J.; Yu, S. S.-F.; Chan, J. C. C. Adsorption of a Statherin Peptide Fragment on the Surface of Nanocrystallites of Hydroxyapatite. *J. Am. Chem. Soc.* **2008**, *130*, 2862–2868.

(33) Dong, X.; Wang, Q.; Wu, T.; Pan, H. Undestanding Adsorption−Desorption Dynamics of BMP-2 on Hydroxyapatite (001) Surface. *Biophys. J.* **2007**, *93*, 750–759.

(34) Capriotti, L. A.; Beebe, T. P., Jr.; Schneider, J. P. Hydroxyapatite Surface-Induced Peptide Folding. *J. Am. Chem. Soc.* **2007**, *129* (16), 5281–5287.

(35) Corno, M.; Busco, C.; Bolis, V.; Tosoni, S.; Ugliengo, P. Water Adsorption on the Stoichiometric (001) and (010) Surfaces of Hydroxyapatite: A Periodic B3LYP Study. *Langmuir* **2009**, *25*, 2188–2198.

(36) Bellamy, L. J. *The Infrared Spectra of Complex Molecules*, 3rd ed.; Chapman and Hall: London, 1975.

(37) Suzuki, S.; Shimanouchi, T.; Tsuboi, M. Normal Vibrations of Glycine and Deuterated Glycine Molecules. *Spectrochim. Acta* **1963**, *19* (7), 1195–1208.

(38) Dovesi, R.; Saunders, V. R.; Roetti, C.; Orlando, R.; Zicovich-Wilson, C. M.; Pascale, F.; Civalleri, B.; Doll, K.; Harrison, N. M.; Bush, I. J., et al. *CRYSTAL06 User's Manual* University of Torino: Torino, Italy, 2006.

(39) Rimola, A.; Zicovich-Wilson, C. M.; Dovesi, R.; Ugliengo, P. Search and Characterization of Transition State Structures in Crystalline Systems Using Valence Coordinates. *J. Chem. Theory Comput.* **2010**, *6* (4), 1341–1350.

(40) Linder, R.; Seefeld, K.; Vavra, A.; Kleinermanns, K. Gas Phase Infrared Spectra of Nonaromatic Amino Acids. *Chem. Phys. Lett.* **2008**, *453*, 1–6.